Manuscript received Sep. 17, 2007; revised Nov. 18, 2007

Automatic Gain Control for Unity Feedback Control Systems with Large Parameters Variations

Tain-Sou Tsay
Department of Aeronautical Engineering,
National Formosa University,
64, Wen-Hwa Road, Huwei, Yunlin, 63208,
Taiwan
tstsay@nfu.edu.tw

Abstract:- In this paper, an automatic gain control scheme is first proposed for analyses and designs of unity feedback control systems. The controlled system is a nonlinear feedback control system. The overall system is equivalent to a conventional automatic gain control loop with command tracking error input. Therefore, it gives good command tracking behaviour while keeping robust characteristic of the original AGC loop. Furthermore, it gives good robustness for coping with fast large parameter variations. The stability and effective of controlled systems are verified by time responses, frequency responses, and parameter variation testing with three numerical examples. Comparisons are also made with the PID control.

Key-Words: - Automatic gain Control, nonlinear feedback System.

1 Introduction

Command tracking error control techniques are well-developed for unity feedback control systems. In this paper, a command tracking error square control scheme is first proposed. It can be rearranged with a fast and a slow command tracking error control loops. The slow loop is used for gain adapting. The fast loop is used for command tracking. The overall system is equivalent to a conventional Automatic Gain Control (AGC) loop [1-9] with command tracking error input. Therefore, it will give good command tracking behavior while keeping robust characteristic of the original AGC loop, especially for the system with fast large parameter variations. For a real application example, load disturbance of servo actuator of a Computer Numerical Control (CNC) machine is often changed abruptly. It implies that high gain-crossover frequency for coping with fast load changing is needed and high gain and phase margins are needed for coping with large load changing. These requirements often increase the system cost. Another possible way is to use adaptive control algorithm [10]. According to the operating condition, parameters of the controller are adjusted. It is effective but complicated. The technique to identify or measure the operational condition is complicated. Furthermore, the adaptation may not fast enough for coping with fast load changing. Another possible controller is the PID controller [11-13]. The PID controllers have been used widely in industry due to robustness and simplicity. It is well known that PID controllers have dominated applications for 60 years, though there has been a lot of interest in research into and implementation of advanced controllers. However, it will be seen that the PID controller with fixed parameters still give bad robustness for coping with fast large load changing. Therefore, parameter adaptation is needed also for PID controller. The same problem may occur for other design techniques.

A simple and effective control technique is usually expected to cope with fast changed large load disturbance. This is the motivation of this paper. For unit feedback control system, gain or phase changing of the plant due to load disturbance presented in command tracking error can not be clearly classified. They can be viewed roughly as loop gain changing of the feedback control system. The magnitude of the tracking error is used as information data for gain adapting in the AGC loop. It will be seen that the large tracking error, the large bandwidth of the AGC loop will be. Therefore, the bandwidth of the AGC loop is adjusted automatically. It implied that loop gain of the controlled system is adjusted automatically and need not extra parameters adaptation for coping with system parameter variations.

Analyzing techniques and stability of the AGC loop are well developed for variations of receiving radio and video signals [1-9]. In this paper, the

stability of the controlled system with the proposed control will be verified by linearized systems. The linearized system is found form the steady-state condition [14, 15]; i.e., equilibrium point. This is similar to all nonlinear systems with conventional linear analyses and design techniques. The suitability of the linearization will be verified by frequency responses of the controlled nonlinear system. Other digital simulations with large parameter variations will be made also to show the performance and robustness.

In following sections, operating theorem of the proposed control scheme is discussed first, and then applied to a simple numerical example to explain designing and linearizing procedures, applied to a rolling flight control system [16-18] to cope with aerodynamic coupling and finally applied to a complicated electro-hydraulic velocity servo system [19,20]. Comparisons will be made with the PID control in analyses and designs of the electro-hydraulic velocity servo system. From simulation results with large gain and phase variation testing, it will be seen the proposed control scheme provides an effective and simple way to get good robustness and performances.

2 The Proposed Method

Consider the control law described by the following equation:

$$C = P(s)F(s)e^2 sign(e) \tag{1}$$

where P(s) is the plant to be controlled, F(s) is the controller, R is the reference command, C is the plant output, e is the command tracking error*(R-C)*, and sign(e) is the sign of e. The sign(e) is used to keep self-consistent for $\lim_{s\to 0} P(s)F(s) \geq 0$. Since F(s) is a selected controller, the condition $\lim_{s\to 0} P(s)F(s) \geq 0$ will usually exist. Eq.(1) can be rewritten as in the form of

$$\begin{aligned} C &= P(s)F(s)e \cdot e \cdot sign(e) \\ &= P(s)F(s)e|e| \\ &= P(s)F(s)(R-C)|R-C| \end{aligned} \tag{2a}$$

and Eq.(2a) can further be rewritten as in the form of

$$\begin{aligned} C &\equiv P(s)[K(s)(R-C)][H(s)|R-C|] \\ &\equiv P(s)[V_i][V_c] \equiv P(s)[Vo] \end{aligned} \tag{2b}$$

where $H(s)K(s) \equiv F(s)$, $V_i \equiv K(s)(R-C)$, $V_c \equiv H(s)|R-C|$, and $V_o \equiv V_i V_C$. Eq.(2b) is realized and shown in Fig.1a. It becomes an AGC loop with V_i and V_c. Note that the system described by Fig.1a without K(s) is equivalent to the conventional Automatic Gain Control (AGC) loop for processing radio or video signal[1-9]. V_i is the receiving signal for processing. R is the wanted signal output level; e.g., wanted contrast or brightness of a picture. Eqs.(1), 2(a), and (2b) can be rewritten also as

$$C = \begin{cases} +P(s)K(s)H(s)(R-C)^2 & for\ R \geq C \\ -P(s)K(s)H(s)(R-C)^2 & for\ R < C \end{cases} \tag{3}$$

Eq.(3) represents that there are two symmetrical control modes. $R-C=0$ is the control purpose and the switching line for mode changing. For simplicity, the control mode for $R \geq C$ will be analyzed only and the overall system includes the control mode for $R < C$ will be verified by digital simulations [20].

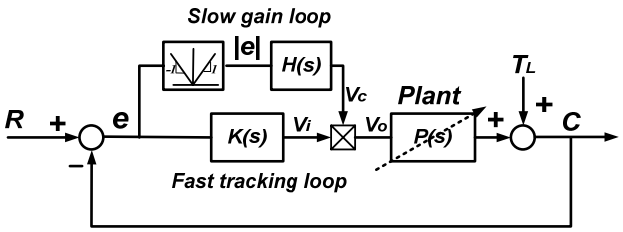

Fig.1a. The proposed command tracking error square control scheme.

Relationships between V_i, V_c, R, and V_o with *P(s), H(s),* and K(s) are given below:

$$\begin{aligned} V_o &= V_i V_c \\ &= [1 + H(s)P(s)V_i]^{-1} H(s)V_i R \end{aligned} \tag{4}$$

and the plant output C with respect to *e,* V_i, and V_c is in the form of

$$\begin{aligned} C &= [1 + H(s)P(s)K(s)e]^{-1} H(s)P(s)K(s)eR \\ &= [1 + H(s)P(s)V_i]^{-1} H(s)P(s)V_i R \\ &= [1 + K(s)P(s)V_c]^{-1} K(s)P(s)V_c R \end{aligned} \tag{5}$$

alternately. Substituting command tracking error e in Eq.(5) with (*R-C*), one has

$$C = [1 + H(s)P(s)K(s)(R-C)]^{-1} H(s)P(s)K(s)(R-C)R \tag{6}$$

From Eqs.(5) and (6), the command tracking error signal e is in the form of

$$\begin{aligned} e &= [1 + H(s)P(s)K(s)e]^{-1} R \\ &= [1 + H(s)P(s)V_i]^{-1} R \\ &= [1 + K(s)P(s)V_c]^{-1} R \end{aligned} \tag{7}$$

alternately, V_i and V_c are in the form of

$$V_c = H(s)e = [1 + K(s)P(s)V_c]^{-1} H(s)R \tag{8}$$

and

$$V_i = K(s)e = [1 + H(s)P(s)V_i]^{-1} K(s)R \tag{9}$$

In general, the magnitude of the loop gain $|H(j\omega)P(j\omega)|$ is very large below the middle frequency band. Eq.(9) can be approximated as $V_i \cong \sqrt{K(s)R/H(s)P(s)}$, and then Eq.(6) can be approximated as

$$T(s) = C/R \cong \left[1+\sqrt{H(s)P(s)K(s)R}\right]^{-1}\sqrt{H(s)P(s)K(s)R} \quad (10)$$

It is similar to linear unity feedback control systems except that it becomes input dependent and the loop transfer function is replaced by its square root. Note that the large value of *R,* the large bandwidth will be. This is the basic characteristic of the AGC algorithm. Note also that Eq.(10) is not analytic form. Therefore, linearizied model of the considered system is needed for analyses and designs.

Now, other formulas are evaluated for finding steady-state conditions of the controlled system. Assume that *K(s), H(s),* and *P(s)* are represented by minimal rational polynomial realizations; i.e., $K(s) \equiv N_K(s)/D_K(s)$, $P(s) \equiv N_P(s)/D_P(s)$ and $H(s) \equiv N_H(s)/D_H(s)$, respectively. Then Eqs.(7) to (9) can be rewritten as in the form of

$$N_K(s)N_H(s)N_P(s)e^2 + D_K(s)D_H(s)D_P(s)e - D_K(s)D_H(s)D_P(s)R = 0 \quad (11)$$

$$D_K(s)N_H(s)N_P(s)V_i^2 + D_K(s)D_H(s)D_P(s)V_i - N_K(s)D_H(s)D_P(s)R = 0 \quad (12)$$

$$N_K(s)D_H(s)N_P(s)V_c^2 + D_K(s)D_H(s)D_P(s)V_c - D_K(s)N_H(s)D_P(s)R = 0 \quad (13)$$

From Eqs.(11) to (13), steady-state solutions e_s , V_{is} , and V_{cs} with a specified value of *R* can be found by following equations:

$$N_K(0)N_H(0)N_P(0)e^2 + D_K(0)D_H(0)D_P(0)e - D_K(0)D_H(0)D_P(0)R = 0 \quad (14)$$

$$D_K(0)N_H(0)N_P(0)V_i^2 + D_K(0)D_H(0)D_P(0)V_i - N_K(0)D_H(0)D_P(0)R = 0 \quad (15)$$

$$N_K(0)D_H(0)N_P(0)V_c^2 + D_K(0)D_H(0)D_P(0)V_c - D_K(0)N_H(0)D_P(0)R = 0 \quad (16)$$

From Eq.(5), one can find steady-state output C_s with e_s , V_{is} , and V_{cs} . It can be represented as

$$C_s = [D_K(0)D_H(0)D_P(0) + N_K(0)N_H(0)N_P(0)e_s]^{-1} \bullet N_K(0)N_H(0)N_P(0)e_s R \quad (17)$$

$$C_s = [D_H(0)D_P(0) + N_H(0)N_P(0)V_{is}]^{-1}N_H(0)N_P(0)V_{is}R \quad (18)$$

$$C_s = [D_K(0)D_P(0) + N_K(0)N_P(0)V_{cs}]^{-1}N_K(0)N_P(0)V_{cs}R \quad (19)$$

alternately. Since there are eight possible combinations of e_s , V_{is} , and V_{cs} may exist for solving Eqs.(14) to (16), another constrain equations are required. They are above three equations. Three relationship (e_s , V_{cs}), (e_s , V_{is}), and (V_{is} , V_{cs}) are derived by equaling Eqs.(17) and (19), Eqs.(17) and (18), Eqs.(18) and (19), respectively.

Now, consider the existence of the steady-state solutions (e_s , V_{is} , V_{cs}). From Eq.(15), one can see that it becomes V_i independent for $D_K(0)$ equals to zero. From Eq.(16), one can see that it becomes V_c independent for $D_H(0)$ equals to zero. These properties imply that only type-0 controllers *K(s)* and *H(s)* are suitable. Assume the plant *P(s*) is a type-0 system also, then the transfer function of *K(s)*, *H(s)* and *P(s)* can be described by following rational polynomials. They are

$$K(s) = \frac{k_k(1 + b_{1k}s + b_{2k}s^2 + ...)}{1 + a_{1k}s + a_{2k}s^2 + ...} \quad (20)$$

$$H(s) = \frac{k_h(1 + b_{1h}s + b_{2h}s^2 + ...)}{1 + a_{1h}s + a_{2h}s^2 + ...} \quad (21)$$

$$P(s) = \frac{k_p(1 + b_{1p}s + b_{2p}s^2 + ...)}{1 + a_{1p}s + a_{2p}s^2 + ...} \quad (22)$$

Then Eqs.(14) to (16) can be simplified as in the form of

$$k_k k_h k_p e^2 + e - R = 0 \quad (23)$$

$$k_h k_p V_i^2 + V_i - k_k R = 0 \quad (24)$$

$$k_k k_p V_c^2 + V_c - k_h R = 0 \quad (25)$$

A sufficient condition for deriving real solutions of Eqs.(23) to (25) are values of k_k, k_h *and* k_p given in Eqs.(23) to (25) greater than zeros.

Using the found V_{cs} to replace the multiplier shown in Fig.1a, then the overall nonlinear control system can be linearized with respect to steady-state conditions V_{cs} and V_{is} for a specified valued of R. The small signal model around the steady-state condition will be found; i.e.; Eq.(4) can be rewritten as

$$\begin{aligned}(V_{os} + \Delta V_o) &= (V_{is} + \Delta V_i)(V_{cs} + \Delta V_c) \\ &= V_{is}V_{cs} + V_{cs}\Delta V_i + V_{is}\Delta V_c + \Delta V_i \Delta V_c\end{aligned} \quad (26)$$

where ΔV_o , ΔV_i , and ΔV_c are small perturbations of V_o , V_i , and V_c with steady states V_{os} , V_{is} and V_{cs} , respectively. The term $\Delta V_i \, \Delta V_c$ given in Eq.(26) can be neglected for small perturbations, and then Eq.(26) can be rewritten as in the form of

$$\Delta V_o \approx V_{cs}\Delta V_i + V_{is}\Delta V_c \quad (27)$$

Replacing the block for $V_o = V_i V_c$ shown in Fig.1a by Eq.(27), the linearized system is derived. Fig.1b

shows the linearized system. Then, one has

$$C = [1 + (V_{is}H(s) + V_{cs}K(s))P(s)]^{-1}[V_{is}H(s) + V_{cs}K(s)]P(s)\,R \quad (28)$$

and

$$C = \frac{V_{is}D_k(s)N_H(s)N_p(s) + V_{cs}N_k(s)D_H(s)N_p(s)}{D_K(s)D_H(s)D_p(s) + V_{is}D_k(s)N_H(s)N_p(s) + V_{cs}N_k(s)D_H(s)N_p(s)}R \quad (29)$$

The characteristic equation of the linearized system is in the form of

$$\Delta(s) = D_K(s)D_H(s)D_p(s) + V_{is}D_k(s)N_H(s)N_p(s) + V_{cs}N_k(s)D_H(s)N_p(s) \quad (30)$$

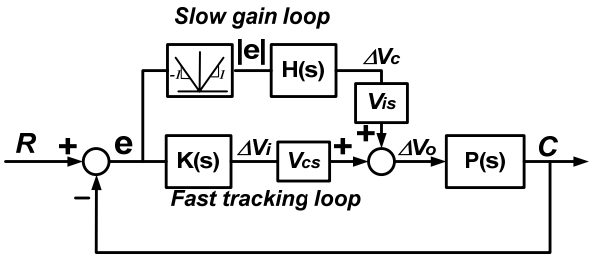

Fig.1b. The linearized control system with steady-state values.

The necessary condition for existence of V_{cs} and V_{is} is to check roots of Eq.(30) are all in left half plane (*LHP*); i.e., it is a stable system. The performance of the closed-loop system is represented by Eq.(29). Eq.(29) will be verified by time responses simulations of the closed loop system shown in Fig.1a with a constant value of the reference input *R* superimposing sinusoidal testing signals.

Summarizing above statements, design procedures are given below [21]:

Step 1: Selecting a desired steady-state tracking error e_s for a specified value of the reference input *R*.

Step 2: Using Eqs.(23)-(25) to find DC gains k_k, k_h and steady-state values of (V_{cs}, V_{is}).

Step 3: Using steady-state values (V_{cs}, V_{is}) to get linearized feedback system described by Eq.(29).

Step 4: Finding frequency elements of *H(s)*, *K(s)* given in Eqs.(20) and (21) to get wanted bandwidth and pole locations in LHP.

Step 5: Simulation verifications with time responses and frequency responses.

Three numerical examples given in next section are used to show advantage of the proposed control scheme.

3 Numerical Examples

For illustration, a simple plant is considered first [20]. It is in the form of

$$P(s) = \frac{10}{1 + 0.5s} \quad (31)$$

Assume that the desired tracking error $e_s = 5\times10^{-3}$ for the command *R*=0.5, then Eq.(23) gives $k_k k_h$=1980 for k_P=10. Selecting $k_k \equiv$40, then one has k_h=49.5. Substituting found value of (k_k, k_h) to Eqs.(24) and (25) with constrains described by Eqs.(17) to (19), one has solutions V_{is}=0.200 and V_{cs}=0.248. Substituting found (k_k, k_h) to Eqs.(23) and (25) for *R*=1, solutions of (e_s, V_{is}, V_{cs}) are (7.1×10^{-3}, 0.283, 0.351). Using found values of (k_k, k_h), controllers can be defined as below:

$$H(s) \equiv \frac{49.5}{1 + \gamma s} \quad (32)$$

and

$$K(s) \equiv 40\,. \quad (33)$$

where γ is a designing parameter. Eq.(32) represents *H(s)* is a low-pass system which slows down the dynamic of V_c. V_c is equivalent to feed-forward gain. Selecting γ=10 and substituting *P(s), K(s),* and *H(s)* to Eq.(30), one has system poles (-0.2, -200.4) for (V_{is}, V_{cs})=(0.200, 0.248), and (-0.2,-281.999) for (V_{is}, V_{cs})=(0.283, 0.35). They are all in left half plane (LHP) and imply that linearized systems are stable and steady-state solutions exist.

Fig. 2 shows closed-loop frequency responses of the linearized system for *R=1*, *5* and *10*; respectively; in which solid-lines show the responses calculated by Eq.(29); dot points show simulation results with constant reference input *R* superimposing sinusoidal signals; i.e., $r(t) = R + A\sin(\omega t)$ to the considered nonlinear system. Steady-state solutions (e_s, V_{is}, V_{cs}) are (7.1×10^{-3}, 0.283, 0.351), (1.6×10^{-2}, 0.635, 0.785), and (2.24×10^{-2}, 0.898, 1.111); respectively. The formula to find gain (M) and phase (ϕ) from time responses is given as

$$T_{simu}(j\omega) = \frac{\int_0^{2\pi/\omega} c(t)e^{-j\omega t}dt}{\int_0^{2\pi/\omega} r(t)e^{-j\omega t}dt} = M\angle\phi \quad (34)$$

where *c(t)* is the time response of system output with input $r(t)$. It can be seen that responses of linearization of the system gives excellent agreement with the considered system.

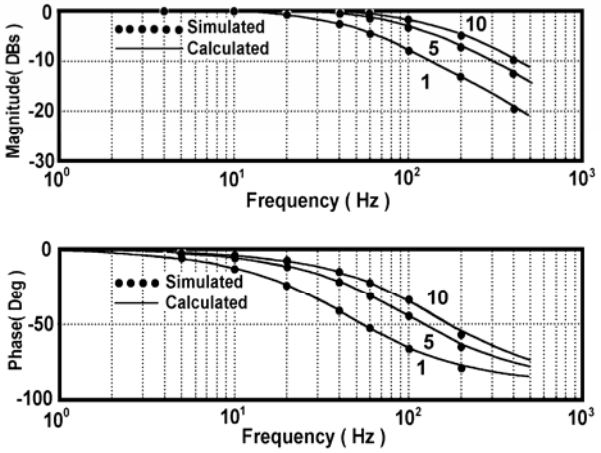

Fig.2. Frequency responses of the closed-loop system.

Fig.3 shows time responses of the controlled system for variable reference inputs *R*; in which *C* represents the system output; V_c represents the control voltage of the inner AGC loop; and V_i represents the input signal of the AGC loop. Fig. 3 shows that the control system is stable regardless of the sign changes of the reference input *R*. This is contrary to the conventional AGC loop, and the performance is nice for the considered system. Note that responses of V_c are dependent upon the bandwidth of the AGC loop. It is controlled by selecting proper feedback controller *H(s)*; described by Eq.(32). The steady-state value V_{cs} is dependent on values of *R*, *K(0)*, *H(0)* and *P(0)*. The large error between input and output is due to the value of V_c does not approach to its steady-state value V_{cs} before 3 seconds; i.e., the duration for *R* =1. Fig. 3 shows the steady-state value V_{cs} = 0.248 for *R*= 0.5 and the steady-state error e_s=5x10^{-3}. These values are agree with calculated results for *R*= 0.5.

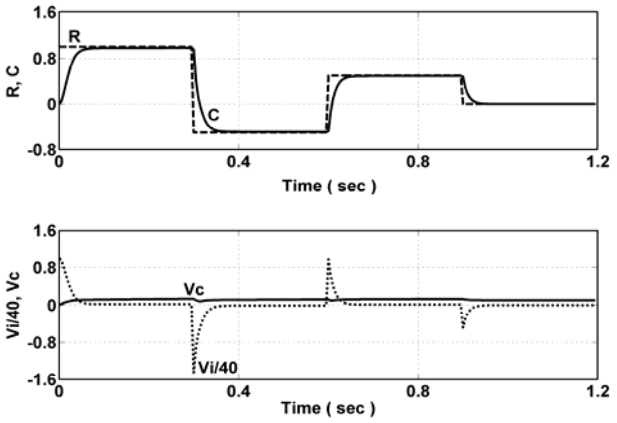

Fig.3. Time responses of the closed-loop system.

Fig.4 shows time responses for the value of *P(0)* varying from 10 to 5 abruptly at time 0.3 seconds, and then varying from 5 to 10 abruptly at time 0.6 seconds, finally varying from 10 to 20 abruptly at time 0.9 seconds. It can be seen that disturbances due to *P(0)* variations are suppressed quickly, and the slowing loop provides suitable gains V_{cs} according to the value of *P(0)* automatically. Note that Figs. 3 and 4 show variations of V_c are much slower than those of $V_i s'$. This is the basic operating behaviors of the conventional automatic gain control loops [14].

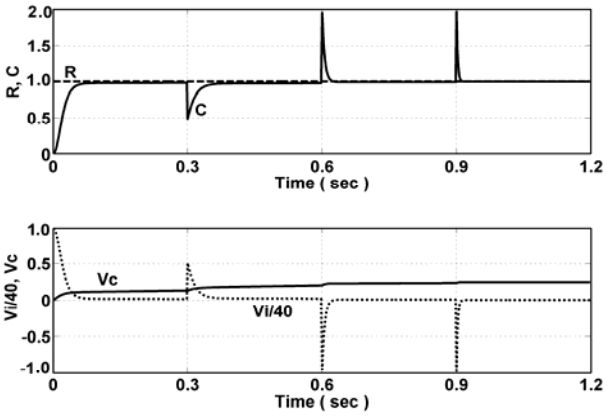

Fig.4. Regulating properties of the closed-loop system with large parameter variations.

Now, consider an aerodynamic coupled rolling flight control system [16-18]. It is a supersonic air-to-air flight vehicle. Fig.5a shows the conventional control configuration, in which K_{op} and K_{ip} are outer and inner loop gains [17]; $L_{\delta p}$ and L_p are aerodynamic coefficients of the rolling dynamics; L_α and L_β are aerodynamic coupling from pitching and yawing channels; α and β are angles of attack and sideslip; p and ϕ are rolling angular rate; and rolling angles, ϕ_c is the rolling command, $\boldsymbol{P_c}$ is the angular rate command. The rolling angle command is always set to be zero for skid to turn (STT) flight vehicle. For Bank to turn (BTT) flight vehicle, rolling angle command is not always zero. There are two summing points show the aerodynamic and kinematic couplings from pitching and yawing channels to the rolling channel. Values of coefficients are $L_{\delta p}$ =15609, L_p =-3.800, L_α=684.5, $L_\beta = 8551.6$ [17]. The loop gain of loop gains K_{op}=49.2175 and K_{ip}=0.0054 [17]. The value of the aerodynamic coupling is always much greater than that of kinematic coupling. Therefore, only the

aerodynamic coupling will be discussed in next paragraph. Fig.5b shows the proposed AGC loop used in inner loop to cope with aerodynamic coupling. Note that another AGC loop can be used also in the outer loop.

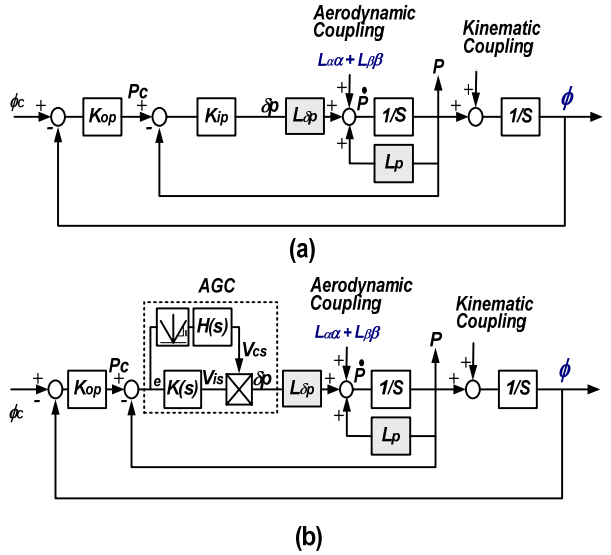

Fig.5 Rolling flight control system (a) the conventional scheme, (b) the proposed scheme.

Assume that the desired tracking error $e_s = 1\times10^{-2}$ for the command P_c=1.0, then Eq.(23) gives $k_k k_h$ =2.4102 for k_P =4107.6. Selecting k_k ≡2.0, then one has k_h =1.2051. Substituting found value of (k_k,k_h) into Eqs.(24) and (25) with constrains described by Eqs.(17) to (19), one has solutions V_{is} =0.020 and V_{cs} =0.0121. Table 1 gives steady-state values (e_s,V_{is},V_{cs}) of another values of P_c. Using found values of (k_k,k_h), controllers can be defined as below:

$$H(s) \equiv \frac{1.2051}{1+\gamma s} \tag{35}$$

and

$$K(s) \equiv 2.00\,. \tag{36}$$

Using steady-state values given in Table 1, pole locations of linearized systems are given in Table 1 for $\gamma = 10.0$. From Table 1, one can see that the large value of P_c, the less value of one pole of the linearized system. This implies that the large value of P_c, the large bandwidth will be. After the outer loop closed with K_{op}, then comparisons between the conventional method and the proposed method can be made to show merit of the proposed method.

The coupling term $L_\alpha\alpha + L_\beta\beta$ is added to the system. Low-pass filters 6.28/(s+6.28) are used to emulate dynamics of pitching and yawing channels; i.e., filtering α and β. Fig.6 shows simulating results of the conventional and the proposed methods with $\alpha = 12°$ and $\beta = 1°$ between 3 and 5 seconds, and $\alpha = -12°$ and $\beta = -1°$ between 7 and 9 seconds. The rolling command is 5.73 degrees between 0 and 2seconds. This period is used to check the performance of the rolling loop only. They show that both of two methods give good compatible results. Therefore, following comparisons can be made. Note that the rolling command is always set to be zero for skid-to-turn flight vehicle. Fig.6 gives the maximal rolling angle is 24.9° and maximal angular rate is 133.06°/s under the coupling added with the conventional control schemes applied. For the proposed method applied, the maximal rolling angle is 1.38° and maximal angular rate is 6.279°/s. Therefore, the proposed method gives better results for coping with aerodynamic coupling than that of the conventional method.

Table 1. Steady-State Values and Poles of linearized Systems.

P_c	V_{is}	V_{cs}	e_s	Poles	
0.10	0.0063	0.0038	0.0031	-121.385	-0.1939
0.50	0.0141	0.0085	0.0071	-269.163	-0.1972
1.00	0.0200	0.0121	0.0100	-379.900	-0.1981
2.00	0.0283	0.0171	0.0142	-536.512	-0.1986
3.00	0.0347	0.0209	0.0174	-656.684	-0.1989
4.00	0.0401	0.0242	0.0201	-757.994	-0.1990
5.00	0.0448	0.0270	0.0224	-847.250	-0.1991

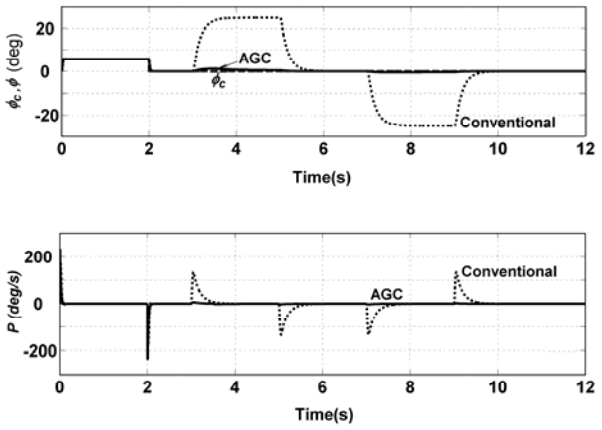

Fig.6. Simulation comparison between conventional and the proposed control scheme.

Now, consider a complicated electro-hydraulic velocity servo system [19, 20] shown in Fig. 7 with system parameters given below:

$K_S = 2.3\times10^{-7}\sqrt{P_S - sign(X_V)P_L}\ m^2/s$; $P_S = 1.4\times10^7\ N_t/m^2$; $\beta_o = 3.5\times10^7\ N_t/m^2$; $V_t = 3.3\times10^{-5}\ m^2/rad$;

C_{tp}=2.3×10^{-11} $m^5/s/N_t$; D_m=1.6× 10^{-5} m^3/rad; J=5.8×10^{-3} Kg-m-s^2; B_m=0.864 $Kg\cdot m\cdot s/rad$; K_v= 0.5 m/v

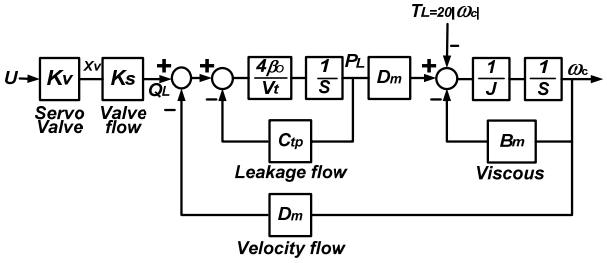

Fig.7. Mathematical Model of an electro-hydraulic velocity Servo-system.

The objective of the control is to keep the velocity ω_c of the hydraulic system following the desired reference input. The relation between the valve displacement X_V and the load flow rate Q_L is governed by the well-known orifice law [20]:

$$Q_L = X_V K_j \sqrt{P_s - sign(X_V)P_L} = X_V K_s ; \quad (37)$$

where K_j is a constant for specific hydraulic motor; P_S is the supply pressure; P_L is the load pressure and; K_S is the valve flow gain which varies at different operating points. The following continuity property of the servo valve and motor chamber yields

$$Q_L = D_m\omega_c + C_{tp}P_L + (V_t - 4\beta_o)\dot{P}_L Q_L; \quad (38)$$

where D_m is the volumetric displacement; C_{tp} is the total leakage coefficient; V_t is the total volume of the oil; β_o is the bulk modulus of the oil; and we is the velocity of the motor shaft. The torque balance Eq.(for the motor is in the form of

$$D_m P_L = J\dot{\omega}_c + B_m\omega_c + T_L ; \quad (39)$$

where B_m is the viscous damping coefficient and T_L is the external load disturbance which is assumed to be dependent upon the velocity of the shaft or slowly time varying as described by T_L =20|ω_c|.

The considered system is a nonlinear system for the load flow rate Q_L is a nonlinear function of the valve displacement X_V and the load pressure P_L. Similar to the design procedure given above, Eq.(23) gives $k_k k_h = 7863$ for $k_P = 7.9168$ and tracking error e_s is chosen as 4×10^{-3} with the command R=1.0. Selecting $k_k \equiv 100$, then one has $k_h = 78.63$ and $V_{is} = 0.3999$ and $V_{cs} = 0.3145$. Controllers can be defined as $H(s) = 78.63/(1+\gamma s)$ and $K(s) = 100$. Eq.(30) gives characteristic roots of the linearized system around (V_{is}, V_{cs})=(0.3999, 0.3145) are (-0.1997, $-1.021\times10^4 \pm j7.368\times10^3$) for γ=10. Using found values of (k_k, k_h), steady values of (e_s, V_{is}, V_{cs}) are (8.95×10^{-3},0.895, 0.704) and (1.27×10^{-2}, 1.267, 0.996) for R=5.0 and 10.0, respectively. Characteristic roots of the controlled system are (-0.1999, $-1.021\times10^4 \pm j1.581\times10^4$) and (-0.1999, $-1.021\times10^4 \pm j1.992\times10^4$). For different values of R, one can find one pole is fixed at -0.1999, real parts of other complex pole pair are fixed at -1.021×10^4 even when R approaches to infinite. Those give linearized systems are all stable. Step responses of the controlled system with different load disturbance T_L are shown in Fig. 8. Variations of the disturbance T_L versus time are given below:

T_L = 20 | ω_c |Kg-m, 0.0s < t < 0.2s;
= 10 | ω_c |Kg-m, 0.2s < t < 0.4s;
= 5 | ω_c |Kg-m, 0.4s < t < 0.6s;
= 0 Kg-m, 0.6s < t < 0.8s.

Fig.8 shows that disturbances due to T_L variations are suppressed quickly, and the output ω_c tracks the reference input R after the control voltage V_c approaches its steady-state value V_{cs}.

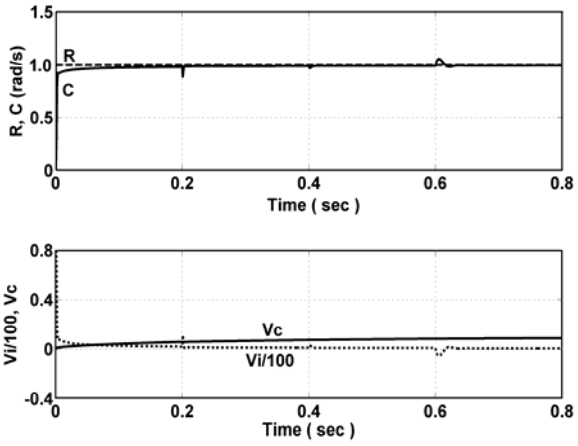

Fig.8. Time responses of the controlled electro-hydraulic velocity servo-system with large load disturbance.

Fig.9 shows comparisons between time

responses of the proposed method and those of the PID control. The PID controller for the electro-hydraulic velocity servo system is in the form of

$$K_{pid}(s) = 0.011 + 37.5/s + 0.078s/(0.2s+1) \quad (40)$$

Parameters of the PID controller are found by optimization method to meet the response of the proposed method for comparing purpose. The solid-lines in Fig.9 show time responses of the system controlled by the proposed controller and doted-lines show time responses of the system controlled by the PID controller. Variations of the disturbance T_L versus time are given in the last paragraph. They are changed abruptly at time 0.2s, 0.4s, and 0.6s. Fig.9 shows that the PID controller is bad for coping with variations of disturbance T_L . Note that performance of the PID control may be better than that of the proposed control before 0.2s, but it gives bad robustness than that of the proposed control after 0.2s. Plant input U shows the equivalent DC gain the plant is increasing. It is due to load changed. Since the proposed method has automatic gain control characteristic, therefore it can give better robustness than that of the PID control. A possible way to improve robustness of the PID control is to use adaptive parameters. They are according with the value of T_L . On-line computing and tuning for PID controls are generally applicable for slow industry processes and can be retuning [11-13]. However, it is not applicable for fast processes or processes with fast parameter variations. This statement will be proven by checking robustness of the system with slow changed load disturbances.

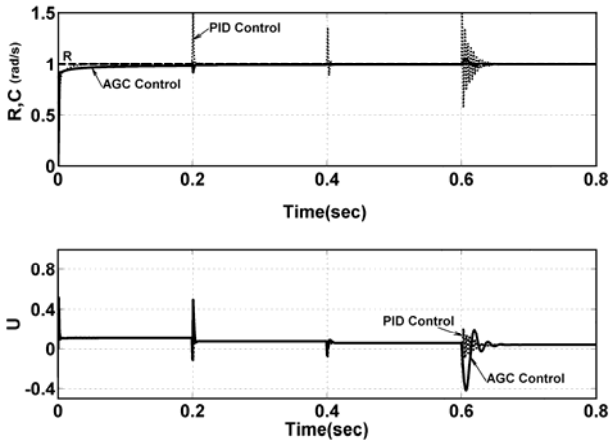

Fig.9. Comparisons between AGC control and PID control with fast changed large load disturbance.

Fig.10 shows time response with slow variations of load disturbance, which is described by

$$T_L = \begin{cases} 20|\omega_c|, & t \le 0.2s \\ [20 - 20(t-0.2)/0.6]|\omega_c|, & t > 0.2s \end{cases} \quad (41)$$

The variation of T_L is decreased slowly to zero. The solid-lines in Fig.10 show time responses of the system controlled by the proposed controller and doted-lines show time responses of the system controlled by the PID controller. Fig.10 shows that both of the proposed control and PID control are robust for coped with slow changed load disturbances. However, Fig.9 shows large difference of them with fast changed load disturbance. It shows that the proposed method has better robustness for coping with fast changed load disturbance.

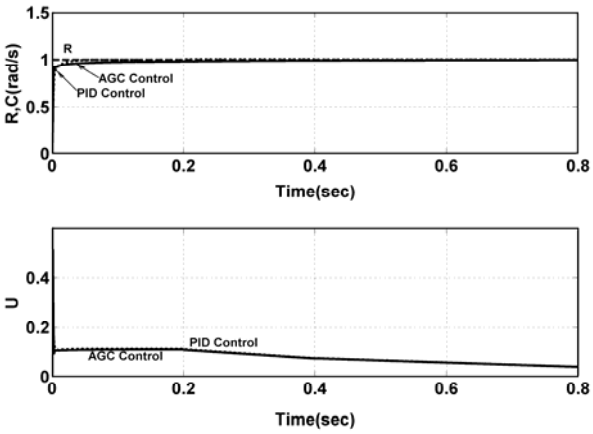

Fig.10. Comparisons between AGC control and PID control with slow changed large load disturbances.

4 Conclusion

In this paper, an automatic gain control scheme has been proposed for analyses and designs of unity feedback control systems. It kept robust properties of the AGC loop while getting good command tracking performance. The systematic analysis and design procedures were presented. The considered systems were a numerical example, an aerodynamic coupled rolling flight control system, and a complicated nonlinear electro-hydraulic velocity servo system. Simulation results with fast large parameter variations were made to show the proposed method could provide an effective and simple way for feedback control systems, especially for coping with large and fast parameters variations.

Furthermore**,** the aerodynamic coupled rolling flight control system design results give that the proposed method has the capability to be applied to large flight envelope operating flight vehicles. They are fast large parameter variation multivariable feedback control systems.

References:

[1] E. D. Banta, Analysis of an automatic gain control (AGC), IEEE Trans. on Automatic Control, AC-9, 1964, pp.181-182.

[2] J. E. Ohlson, Exact dynamics automatic gain control, IEEE Trans. on Communications, 1974, pp.72-75.

[3] A. Guesalaga and S. Tepper, Synthesis of automatic gain controllers for conical scan tracking Radar, IEEE Trans. on Aerospace and Electronic Systems, Vol.36, 2000, pp.302-309.

[4] Y. Zhen, Adaptive integrated RF transceivers for wireless communication: invited paper, Proceeding of the 5th WSEAS International Conference on Mathematical Method and Computational Techniques in Electrical Engineering, Vouliagmeni, Greece, Dec. 29-31, 2003,pp.1-8.

[5] D. V. Mercy, A review of automatic gain control theory, Electron Radio Engineers, Vol. 51, 1981, pp.579-590.

[6] T. J. Shan and T. Kailath, Adaptive algorithms with an automatic gain control feature, IEEE Trans. on Circuits and Systems, Vol.35, 1988, pp.122-125.

[7] D. N. Green, Global stability analysis of automatic gain control circuits, IEEE Trans. on Circuits and Systems, Vol.30, 1983, pp.78-83.

[8] D. M. Badger, Stability of AGC circuits containing peak detectors, IEEE Trans. on Consumer Electronics, Vol.38, 1992, pp.377-383.

[9] K. R. Fowler, Automatic gain control for image-intensified camera, IEEE Trans. on Instrumentation and Measurement, Vol.53, 2004, pp.1057-1064.

[10] S. Sastry and M. Bodson, Adaptive control-stability, convergence, and robustness, Prentice- Hall International Inc., New Jersey, 1994.

[11] K. J. Åström and T. Hägglund, Automatic tuning of simple regulators with specifications on phase and amplitude margins, Automatica, Vol.20, 1984, pp.645-651.

[12] K. J. Åström and T. Hägglund, PID Controllers: Theory, Design, and Tuning, 2nd Edition, Instrument Society of America, 1995.

[13] K. J. Åström and C. C. Hang, Towards intelligent PID control, Automatica, Vol. 28, No.1, 1991, pp.1-9.

[14] R. W. Newecomb, Nonlinear system analyses, Prentice-Hall International Inc., New Jersey, 1978.

[15] J. J. E. Slotine and W. Li, Applied nonlinear control, Prentice-Hall International Inc., New Jersey, 1991.

[16] W. J. Monta, Supersonic Aerodynamic Characteristics of A Sparrow III Type Missile Model With Wing Control and Comparison With Existing Tail-control Results, NASA-TR-1078, Langley Research Center, Hompton, Virginia, 1977.

[17] T. S. Tsay, Linear Quadratic Regulation Method for Supersonic Missile Flight Control System Design, Journal of Aeronautics, Astronautics and Aviation Series A, Vol.38, No.3, 2007, pp.207-216.

[18] T. Kamuran and J. M. Elbrous, H∞ loop shaping robust control vs. classical PI(D) control: A case study on the longitudinal dynamics of Hezarfen UAV, Proceeding of the 2nd WSEAS International Conference on Dynamical Systems and Control, Bucharest, Romania, Oct. 16-17, 2006, pp.105-110.

[19] T. L. Chern and Y. C. Wu, Design of integral variable structure controller and application to electro-hydraulic velocity servo-systems, PROC. IEE, Pt.D, Vol.138, 1991, pp.439-444.

[20] H. E. Merrit, Hydraulic control system, John Wiley, New York, 1976.

[21] T. S. Tsay, Analysis and design of feedback control systems with tracking errors square, Asian J. Control, Vol.9, No.3, 2007, pp.333-339.